Analyst

ROYAL SOCIETY OF CHEMISTRY

PAPER

View Article Online
View Journal | View Issue

Cite this: *Analyst*, 2021, **146**, 2229

Highly selective simultaneous determination of Cu(II), Co(II), Ni(II), Hg(II), and Mn(II) in water samples using microfluidic paper-based analytical devices†

Pornphimon Kamnoet,[a] Wanlapa Aeungmaitrepirom, *[a] Ruth F. Menger [b] and Charles S. Henry *[b]

A new paper-based analytical device design was fabricated by a wax printing method for simultaneous determination of Cu(II), Co(II), Ni(II), Hg(II), and Mn(II). Colorimetry was used to quantify these heavy metal ions using bathocuproine (Bc), dimethylglyoxime (DMG), dithizone (DTZ), and 4-(2-pyridylazo) resorcinol (PAR) as complexing agents. The affinity of complexing agents to heavy metal ions is dependent on the formation constant (K_f). To enhance the selectivity for heavy metal ion determination, the new device was designed with two pretreatment zones, where masking agents remove the interfering ions. It was found that two pretreatment zones worked better than a single pretreatment zone at removing interferences. The reaction time, sample and complexing agent volumes, and complexing agent concentrations were optimized. The analytical results were achieved with the lowest detectable concentrations of 0.32, 0.59, 5.87, 0.20, and 0.11 mg L^{-1} for Cu(II), Co(II), Ni(II), Hg(II), and Mn(II), respectively. The linear ranges were found to be 0.32–63.55 mg L^{-1} (Cu(II)), 0.59–4.71 mg L^{-1} (Co(II)), 5.87–352.16 mg L^{-1} (Ni(II)), 0.20–12.04 mg L^{-1} (Hg(II)), and 0.11–0.55 mg L^{-1} (Mn(II)). The lowest detectable concentration and linearity for the five metal ions allow the application of this device for the determination of heavy metal ions in various water samples. The sensor showed high selectivity and efficiency for simultaneous determination of Cu(II), Co(II), Ni(II), Hg(II), and Mn(II) in drinking, tap, and pond water samples on a single device and detection with the naked eye. The results illustrated that the proposed sensor showed good accuracy and precision agreement with the standard ICP-OES method.

Received 9th November 2020,
Accepted 24th January 2021

DOI: 10.1039/d0an02200d

rsc.li/analyst

Introduction

Electronic manufacturing facilities and electric power plants are very important and their presence has been continuously growing in developing countries. These industrial facilities, however, release various toxic pollutants that can negatively affect the environment and human health. For example, heavy metals are toxic elements that are released and contaminate water, soil, and air.[1,2] These contaminants do not degrade, resulting in environmental accumulation. Heavy metals are toxic to humans and other living organisms, causing lung damage, neurological and immune disorders, and cancers.[3] The World Health Organization has set the maximum permissible concentrations of Cu(II), Ni(II), Hg(II), and Mn(II) in drinking water as follows: 2.00 mg L^{-1}, 0.07 mg L^{-1}, 0.006 mg L^{-1}, and 0.10 mg L^{-1}, respectively (WHO, 2017). The Ministry of Natural Resources and Environment in Thailand also has set the maximum permissible amount of Cu(II) (2.00 mg L^{-1}), Ni(II) (1.00 mg L^{-1}), Hg(II) (0.005 mg L^{-1}), and Mn(II) (5.00 mg L^{-1}) in industrial effluents.[4] To assess water quality, toxic metals are determined using many conventional methods,[5–7] such as atomic absorption spectrometry (AAS),[8,9] fluorescence spectrometry,[10] and electrochemical methods.[11–13] These techniques are highly selective and sensitive, have low detection limits, and can detect multiple elements simultaneously. However, expensive instrumentation, time-consuming processes, and highly skilled technicians are required. Therefore, the development of selective, sensitive, simple, and low-cost methods has been emphasized for heavy metal detection.

Microfluidic paper-based analytical devices (μPADs) have become a common tool for heavy metal monitoring.[14–17]

[a]*Environmental Analysis Research Unit (EARU), Department of Chemistry, Faculty of Science, Chulalongkorn University, Phayathai Road, Pathumwan, Bangkok 10330, Thailand. E-mail: wanlapa.A@chula.ac.th*

[b]*Department of Chemistry, Colorado State University, Fort Collins, Colorado 80523, USA. E-mail: chuck.henry@colostate.edu*

†Electronic supplementary information (ESI) available. See DOI: 10.1039/d0an02200d

μPADs are low-cost, flexible, absorbent, lightweight, high throughput, and biodegradable, and induce flow without pumps *via* capillary action,[18–22] making them useful for heavy metal quantification in food, clinical, and environmental samples.[23,24] Wax printing techniques are extensively used to fabricate hydrophobic barriers on the paper substrate due to their simplicity and high resolution.[25,26] Colorimetric detection methods with μPADs make analyte detection fast and easy, without external instrumentation.[27] Several previous reports have demonstrated the use of μPADs for toxic metal analysis. For example, a 3D origami paper-based analytical device combined with a PVC membrane was reported for colorimetric Cu(II) determination.[28] A paper strip was integrated with a smartphone for Zn(II), Cr(VI), Cu(II), Pb(II), and Mn(II) colorimetric detection in wastewater.[29] A colorimetric paper sensor based on cation-exchange (belt-like ZnSe nanoframes as the colorimetric reagent) was applied for visual determination of Ag(I), Cu(II), and Hg(II).[30] A multilayer paper-based sensor was designed for electrochemical detection of Cd(II) and Pb(II) and colorimetric detection of Fe(III), Ni(II), Cr(VI), and Cu(II).[31] A colorimetric paper-based device was used for semiquantitative Pb(II) detection with a smartphone.[32] While these paper-based methods have been successful for on-site toxic metal analysis with a smartphone, they can only be used for limited metal ions, require time-consuming processes for reagent synthesis, and suffer from complicated steps, narrow linearity, high error due to variable lighting conditions, and limited application due to the smartphone model.

To improve the limitations of the previous methods, this work focused on the development of a paper-based sensor for simultaneous colorimetric detection of Cu(II), Co(II), Ni(II), Hg(II), and Mn(II). After preparation with optimized masking and complexing agents for the five target metal ions, the paper-based sensor can be used to simultaneously detect Cu(II), Co(II), Ni(II), Hg(II), and Mn(II) with the naked eye. The device design consists of a sample zone, to which the sample solution is added, connected to five sets of pretreatment and detection zones. Masking agents which are added to the pretreatment zones remove the interfering ions and enhance the selectivity, while complexing agents which are added to the detection zones react selectively with the target metal ions to form colored products. It was found that two pretreatment zones worked better than a single pretreatment zone at removing interferences. The colorimetric reactions in the device were analyzed by scanning the device followed by analysis using ImageJ. The proposed paper-based sensor demonstrated highly selective and sensitive detection of Cu(II), Co(II), Ni(II), Hg(II), and Mn(II) with great linearity and low limits of detection in drinking, tap, and pond water samples.

Experimental

Chemicals

The standard solutions of the five target metal ions were copper(II) nitrate trihydrate (Sigma-Aldrich), cobalt(II) chloride (Sigma-Aldrich), mercury(II) chloride (Sigma-Aldrich), nickel(II) sulfate hexahydrate (Alfa Aesar), and manganese(II) chloride tetrahydrate (Chem-Impex International Inc). The interfering ions were potassium nitrate (Sigma-Aldrich), sodium nitrate (Sigma-Aldrich), magnesium chloride hexahydrate (Alfa Aesar), and calcium nitrate tetrahydrate (Alfa Aesar), as common ions found in waters, and cadmium(II) nitrate tetrahydrate (Sigma-Aldrich), lead(II) nitrate (Sigma-Aldrich), zinc(II) nitrate hexahydrate (Sigma-Aldrich), potassium dichromate (Alfa Aesar), iron(III) chloride (Sigma-Aldrich), iron(II) sulfate heptahydrate (Sigma-Aldrich), and vanadium(III) chloride (Sigma-Aldrich) were also studied.

Metal ion solutions were prepared in acetate buffer (0.1 M, pH 5.0). Acetate buffer was prepared by dissolving sodium acetate (Merck) and acetic acid (Sigma-Aldrich) in Milli-Q water (Millipore Milli-Q purification system, $R \geq 18.2$ MΩ cm^{-1}). Complexing agents, masking agents, and all reagents were prepared and used without purification and are shown in Tables S1 and S2.†

Instrumentation

A benchtop pH meter with a glass electrode (Mettler Toledo FE20 FiveEasy Plus ™, Switzerland) was used to measure the pH values of solutions. Inductively coupled plasma-optical emission spectrometry (Thermo Scientific, model iCAP 6500 series ICP-OES Spectrometer) was used as the standard method for validation. Images of the colorimetric paper-based device were obtained using a scanner (Brother MFC-8370DN).

Device design and fabrication

The device was designed using CorelDRAW software. The structural design consisted of the sample zone (13 mm diameter), five detection zones (6 mm diameter), ten pretreatment zones (5 mm diameter), and channels (2 × 3 mm) to connect the zones. The design was printed onto Whatman grade 1 qualitative filter paper using a Xerox Phaser 8860 wax printer.[25] This wax pattern was melted at 200 °C for 30 s using a hot plate, forming three-dimensional hydrophobic barriers as the wax melted into the paper. After heating the device, the dimensions of the printed designs decreased by ~1 mm. The backside of the device was sealed with clear packing tape to prevent the leakage of the solution through the paper during analysis. The device was prepared for simultaneous detection of Cu(II), Co(II), Hg(II), Ni(II), and Mn(II) as follows.

Colorimetric detection and interference studies

Cu detection. A solution of 10 mM bathocuproine (Bc) and 80 mg mL^{-1} polyethylene glycol (PEG 400) was prepared in chloroform. Two 2.0 μL aliquots of hydroxylamine hydrochloride (0.5 g mL^{-1}), 2.0 μL of CH_3COOH/NaCl buffer (10 mM, pH 4.6), and 2.0 μL of bathocuproine/PEG 400 solution were added to detection zone 1. Four 2.5 μL aliquots of NaF (0.5 M) were added to pretreatment zone 1. The device was allowed to dry at room temperature in between each reagent addition.

Co detection. A solution of 5 mM 4-(2-pyridylazo) resorcinol (PAR) and 5% w/w poly(diallyldimethylammonium chloride) (PDDA) was prepared in borate buffer (0.1 M, pH 9.3). Two 2.5 μL aliquots of PAR/PDDA solution were added to detection zone 2. Three 2.5 μL aliquots of ethylenediamine (4 M) were added to pretreatment zone 2. Four 2.5 μL aliquots of EDTA (0.2 M) were added to pretreatment zone 1, followed by four 2.5 μL aliquots of triethylenetetramine (0.4 M). The device was allowed to dry at room temperature in between each reagent addition.

Hg detection. Three 3.0 μL aliquots of PEG 400 (80 mg mL^{-1}) were added to detection zone 3, followed by two 1.5 μL aliquots of dithizone (2 mM). Two 2.5 μL aliquots of ethylenediamine (10 M) were added to pretreatment zone 2. Four 2.5 μL aliquots of 0.1 M *trans*-1,2-diaminocyclohexane-*N*,*N*,*N*′,*N*′-tetraacetic acid (DCTA) were added to pretreatment zone 1, followed by two 2.5 μL aliquots of KCN (0.1 M). The device was allowed to dry at room temperature in between each reagent addition.

Mn detection. A solution of 5 mM PAR and 5% w/w PDDA was prepared in borate buffer (0.1 M, pH 9.3). Two 2.5 μL aliquots of PAR/PDDA solution were added to detection zone 4. Four 2.5 μL aliquots of ethylenediamine (8 M) and four 2.5 μL aliquots of thiourea (1 M) were added to pretreatment zones 2 and 1, respectively. The device was allowed to dry at room temperature in between each reagent addition.

Ni detection. Four 2.0 μL aliquots of hydroxylamine hydrochloride (0.5 g mL^{-1}), two 1.5 μL aliquots of dimethylglyoxime (60 mM, DMG) solution, followed by two 2.0 μL aliquots of ammonium hydroxide (0.03 M) were added sequentially to detection zone 5. Two 2.5 μL aliquots of NaF (0.5 M) were added to pretreatment zone 2, followed by two 2.5 μL aliquots of acetic acid (6.3 M). The device was allowed to dry at room temperature in between each reagent addition.

Analytical procedures for simultaneous metal ion determination. The paper-based devices were prepared with the optimized reagents for each metal. A metal ion solution (300 μL) containing the five metals of interest was added to the sample zone. The solution flowed through the pretreatment zones into the detection zones where the metal underwent a colorimetric reaction with the preloaded complexing agents. After the optimal reaction time (120 min), the device was scanned and the image was saved in the JPEG format. A scanner was used to decrease errors arising from variable external lights. The metal ions were quantified by analyzing the image of the device using the open source software ImageJ (National Institutes of Health). The target metal ion quantification was processed as shown in Fig. 1.

Interference studies. To assess the potential of interfering ions, Cd(II), Zn(II), Pb(II), Fe(II), Fe(III), Cr(VI), and V(III) were studied at 1 : 1 and 1 : 2 ratios of the target metal ion (0.455 mM) to the interfering ion. The effects of alkali and alkaline earth metals (K(I), Na(I), Mg(II), and Ca(II)) were evaluated by varying the ratio of the target metal ion (0.455 mM) to these ion concentrations (1 : 100 and 1 : 1000). The color change in the detection zones of the device was measured using the optimum color channel of each reaction as determined by analysis using ImageJ. The tolerance limit for the interfering ions was defined as <10%.

Optimization conditions for simultaneous detection of the five metal ions

To optimize the effect of metal ion volumes (200–300 μL), reaction times (120–200 min), and volumes of complexing agents (2.0–10.0 μL) on the color intensity response, μPADs were prepared with a single set of reaction conditions for the detection and the pretreatment zones in one device for each metal of interest. The optimal reaction times and complexing agent volumes were evaluated by measuring the color intensity of the detection zones (n = 5). The metal ion volumes were assessed

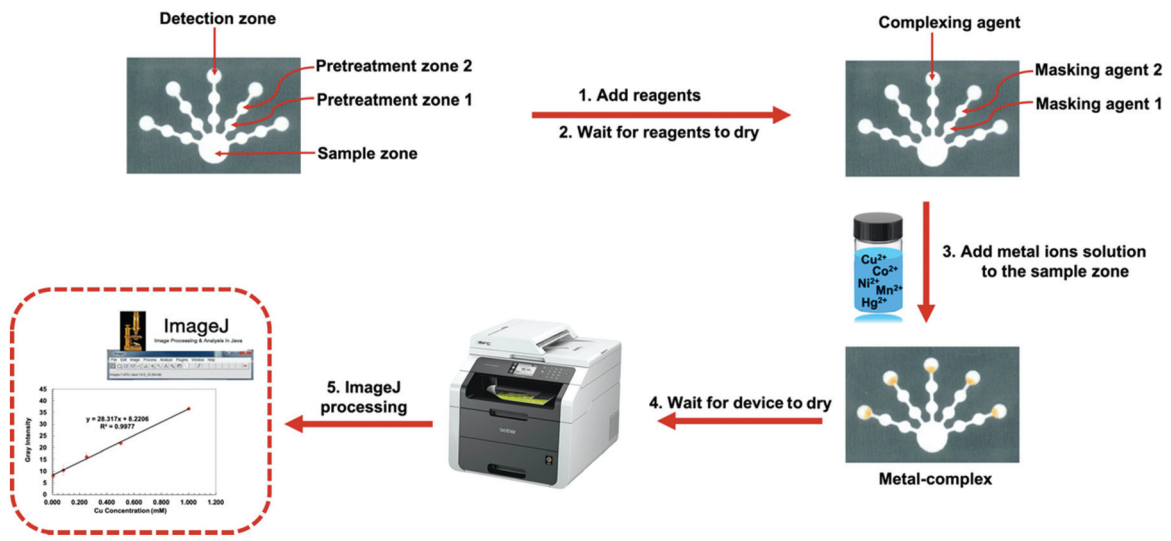

Fig. 1 The process of fabricating μPAD and detecting Cu(II), Co(II), Ni(II), Hg(II), and Mn(II).

by considering the color change of metal complexes in the detection zones.

Image analysis

For colorimetric analysis, the paper-based devices were scanned after the optimum reaction time and the images were saved in the JPEG format at 1200 dpi. The images were processed using ImageJ to determine the color intensity of the detection zones (Fig. S1, ESI†). Each image was inverted and then split into four color channels: grey, red, green, and blue. The circle tool was used to determine an analysis region that had the same size as that of the detection zone. The average intensity of each region was recorded for each color channel. The linear regression equation for each metal reaction was obtained by plotting the color intensity *vs.* target metal concentration. The regression equation and correlation coefficient (R^2) were evaluated to select the optimum color intensity for further studies.

Results and discussion

Device design and fabrication

The proposed paper-based sensor design has a sample zone, 10 pretreatment zones, and 5 detection zones to detect the five target metals. The two pretreatment zones preceding each detection zone were used to (1) increase the area available for reagent and masking agent loading to eliminate interfering ions and (2) decrease the strongly basic effect of ethylenediamine at pH 12.2 (WHO, 1991), which improves the potential of masking agents for Co(II), Hg(II), and Mn(II) analysis. The detection zones contain complexing agents that form colored complexes with the target metal ions. Once the aqueous sample is added to the sample zone, it travels through the paper through the pretreatment zones into the detection zones by capillary action. This device design was applied for simultaneous analysis of the five heavy metal ions using small reagent and sample volumes.

Optimization conditions for simultaneous detection of the five metal ions

Reaction time. The reaction time was optimized in the range of 120–200 min (room temperature) by using a metal ion volume of 300 μL. The color intensities were not significantly different over time for Cu(II), Co(II), Ni(II), Hg(II), and Mn(II) as shown in Fig. S2 (ESI†). For qualitative analysis, the device can be analyzed with the naked eye at reaction times less than 120 min, but it took 120 min for the device to fully dry. A completely dry device is necessary to scan it for quantitative analysis. Therefore, 120 min was selected to optimize other parameters as the paper was completely dry and also maintained the color intensity.

Metal ion volume. As previously optimized with a 300 μL sample volume, the optimal reaction time was 120 min. In order to decrease the reaction time, the sample volume was decreased to 200 and 250 μL; but in these cases, the metal ion solution did not completely flow into the detection zone (reaction time of 120 min) for Mn(II) analysis as illustrated in Fig. S3 (ESI†). The viscosity of 10 M ethylenediamine in the pretreatment zone affected the flow of the aqueous solution through the paper into the detection zone. Therefore, 300 μL of metal ion solution was chosen as the sample volume for further studies and for all metals.

Complexing agent volume. The complexing agent volumes were optimized with 300 μL (metal ion volume) and 120 min (reaction time). The optimal total volumes of Bc (2.0 μL), PAR (5.0 μL), DMG (3.0 μL), DTZ (3.0 μL), and PAR (5.0 μL) were determined for Cu(II), Co(II), Ni(II), Hg(II), and Mn(II) determination, respectively. Due to the size of the detection zone, the optimal total volume of complexing agents was added in multiple smaller aliquots. With low volumes of complexing agent, they did not efficiently react with the metal ions, so the color intensity was not as strong. On the other hand, with too much complexing agent, the change in the color intensity of the detection zone also decreased due to the high background color intensity and high hydrophobicity of some complexing agents in the detection zone (Fig. S4, ESI†). For Cu(II) analysis, 2.0 μL of bathocuproine was selected instead of 4.0 μL because the higher volume of Bc increased the hydrophobicity of the detection zone, obstructing the flow of the metal solution into the detection zone.

Image analysis. Based on the regression equation and correlation coefficient (R^2) results, the gray channel was chosen for Cu(II) and the green channel was selected for Co(II), Ni(II), Hg (II), and Mn(II) analysis (Fig. S5a–e, ESI†).

Colorimetric detection and interference studies

Bathocuproine (Bc) is a sensitive and selective complexing agent commonly used for Cu assay.[33] Bathocuproine–Cu is a strong complex and is stable over a wide range of pH values.[34] Bathocuproine reacts with Cu(I) to form an orange complex[35] (Fig. S2, ESI†). Hydroxylamine hydrochloride (0.5 g mL^{-1}) was added to the detection zone to (1) reduce Cu(II) to Cu(I) and (2) mask interferences from Zn(II), Co(II), and Cd(II).[36] CH_3COOH/NaCl buffer (10 mM, pH 4.6) was loaded to adjust the pH value and stabilize the $Cu(Bc)_2$ complex with the Cl^- anion.[36] Since Bc is hydrophobic and obstructs the flow of aqueous solution into the detection zone, PEG 400 (80 mg mL^{-1}) was mixed with the bathocuproine solution to increase the hydrophilicity of the detection zone. NaF (0.5 M) was added to the pretreatment zone 1 to mask Fe(III) and Co(II).[36] The lowest detectable concentration is defined as the lowest amount of metal that can be reproducibly detected.[36] The lowest detectable concentration based on image analysis for Cu(II) was determined to be 0.005 mM with a linear range of 0.005–1.000 mM (Fig. 2).

Dithizone (DTZ)–Hg complex has a strong interaction with a formation constant of $\log K_f$, Hg-$(DTZ)_2$ = 40.3.[37] DTZ forms different colored complexes with metal ions at various pH values.[38,39] The structure of the $Hg(DTZ)_2$ complex[40] is shown in Fig. S3 (ESI†). Ethylenediamine (10 M) was used to mask Cu(II), Ni(II), Zn(II), Cd(II), and Pb(II) in pretreatment zone 2.[41–44] DCTA (0.1 M), which masks Cu(II), Co(II), Ni(II), Pb(II),

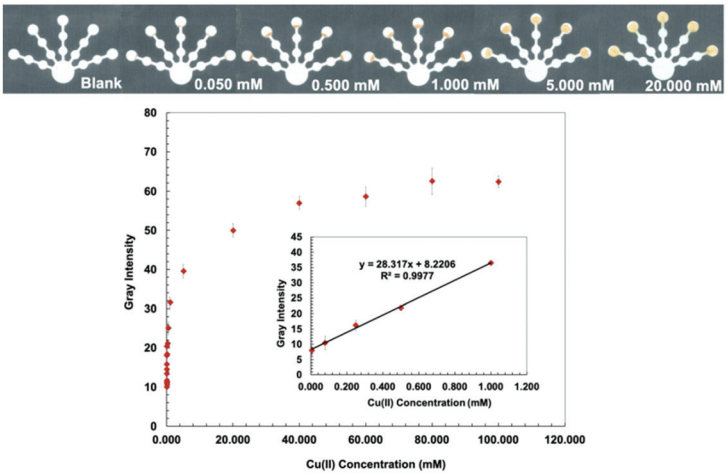

Fig. 2 Visual calibration curve was generated for semi-quantitative Cu(II) determination (top). Cu(II) calibration curve was produced in the range of 0.005–1.000 mM by analyzing the gray intensity of the color change in the detection zone (bottom).

Zn(II), Cr(VI), and Mn(II), and KCN (0.1 M), which masks Cu(II), Co(II), Ni(II), Zn(II), and Cd(II) were added to pretreatment zone 1.[45,46] PEG 400 (80 mg mL^{-1}) was added to the detection zone before loading DTZ to increase the hydrophilicity of the detection zone. Hg conditions show the lowest detectable concentration of 0.001 mM and a linear range of 0.001–0.060 mM (Fig. 3).

4-(2-Pyridylazo) resorcinol (PAR) is frequently applied as an analytical reagent for heavy metal analysis. PAR forms a red-colored complex with numerous metal ions including Cu(II), Co(II), Ni(II), Hg(II), Zn(II), Mn(II), Cd(II), and Pb(II).[47] PAR is a highly selective and sensitive colorimetric reagent for Mn(II), Ni(II), Zn(II), and Pb(II) under strongly basic conditions (pH 11).[48] A PAR/PDDA solution was added to the detection zones for Co(II) and Mn(II) detection ($\log K_f$ (Co(II)–PAR) > 12 and $\log K_f$ (Mn(II)–PAR) = 9.7).[43] PDDA (5% w/w) was mixed with a PAR solution to stabilize and immobilize the metal–PAR complexes.[17] The red $Co(PAR)_2$ and $Mn(PAR)_2$ complex structures[49] are shown in Fig. S4 and S5 (ESI†). For Co(II) detection, ethylenediamine (4 M) was used to mask Cu(II), Ni(II), Zn(II), Cd(II), and Pb(II) in pretreatment zone 2. Triethylenetetramine (0.4 M) and EDTA (0.2 M) were added to pretreatment zone 1 to mask Cu(II), Zn(II), Cd(II), Pb(II) and Mn(II), and Ni(II), Zn(II), Cd(II), Pb(II), and Fe(III), respectively.[49] Co conditions show the lowest detectable concentration of 0.010 mM and a linear range of 0.010–0.080 mM (Fig. 4). For Mn(II) detection, thiourea (1 M),

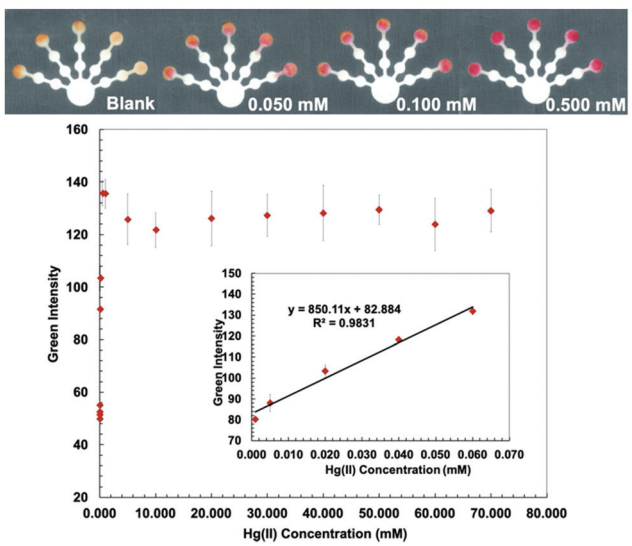

Fig. 3 Visual calibration curve was generated for semi-quantitative Hg (II) determination (top). Hg(II) calibration curve was produced in the range of 0.001–0.060 mM by analyzing the green intensity of the color change in the detection zone (bottom).

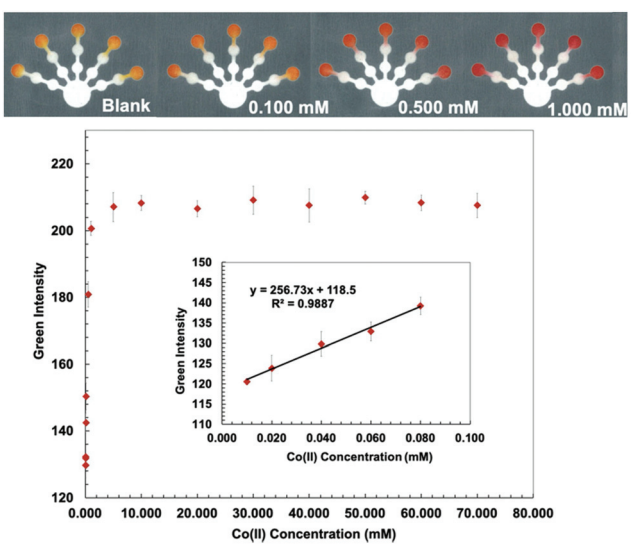

Fig. 4 Visual calibration curve was generated for semi-quantitative Co (II) determination (top). Co(II) calibration curve was produced in the range of 0.010–0.080 mM by analyzing the green intensity of the color change in the detection zone (bottom).

which masks Cu(II), and ethylenediamine (8 M), which masks Cu(II), Ni(II), Zn(II), Cd(II), and Pb(II), were added to pretreatment zones 1 and 2, respectively.[50] Mn conditions show the lowest detectable concentration of 0.0020 mM and a linear range of 0.0020–0.0100 mM (Fig. 5).

Dimethylglyoxime (DMG) is an effective complexing agent that forms a pink colored complex with nickel under basic conditions (Fig. S6, ESI†).[31,51,52] The formation constant (K_f) of the $Ni(DMG)_2$ complex was reported to be $\log K_f = 17.62$.[53] Hydroxylamine hydrochloride (0.5 g mL^{-1}) was added to the detection zone to mask Co(II), Zn(II), and Cd(II).[36] The optimum pH value of the $Ni(DMG)_2$ complex is approximately 9, so the pH value of the detection zone was adjusted with ammonium hydroxide (0.03 M, pH 9.5).[54] To remove the interference from Co(II) and Fe(III), NaF (0.5 M) was added to pretreatment zone 2, followed by acetic acid (6.3 M). Although the conditions in pretreatment zone 2 were strongly acidic, they did not affect Ni complex formation.[36] These conditions resulted in the lowest detectable concentration of 0.100 mM and a linear range of 0.100–6.000 mM for Ni(II) (Fig. 6).

The effect of the interfering ions on each target metal ion (0.455 mM) was evaluated under the optimized reagent conditions. The interfering ions in the target group (Cu(II), Co(II), Ni(II), Hg(II), and Mn(II) as binary solutions and as a mixed solution of the five metal ions which is called All-5) were studied by varying the concentrations in the ratios of 1 : 1 and 1 : 2. Other metal interferences including Cd(II), Zn(II), Pb(II), Fe(III), Fe(II), Cr(VI), and V(III) were also assessed at the ratios of 1 : 1 and 1 : 2. Alkali and alkaline earth metals were evaluated at the ratios of 1 : 100 and 1 : 1000. The tolerance limit is defined as the ion concentration which causes a relative error of target ion analysis of less than ± 10%.[14]

At 1 : 1 ratio, there were no interferences between the target metal ion and any of the other metals (Fig. S6 and S7, ESI†). For Cu(II), Co(II), Hg(II), and Mn(II) detection, there was no interference at the 1 : 2 ratio between the target metal ion and the other metals, except for Ni(II) detection (Fig. S8 and S9, ESI†), where 0.910 mM Co(II) interfered and caused a relative error of 13.19% (Fig. S9C†). At 100 times K(I), Na(I), Mg(II), and Ca(II) did not interfere with Cu(II), Co(II), Ni(II), Hg(II), and Mn (II) detection (Fig. S10, ESI†). Moreover, K(I), Na(I), Mg(II), and Ca(II) at the ratio of 1000 : 1 did not interfere with Co(II) determination and Na(I) at the ratio of 1000 : 1 did not interfere with Ni(II) determination (Fig. S10B, ESI†).

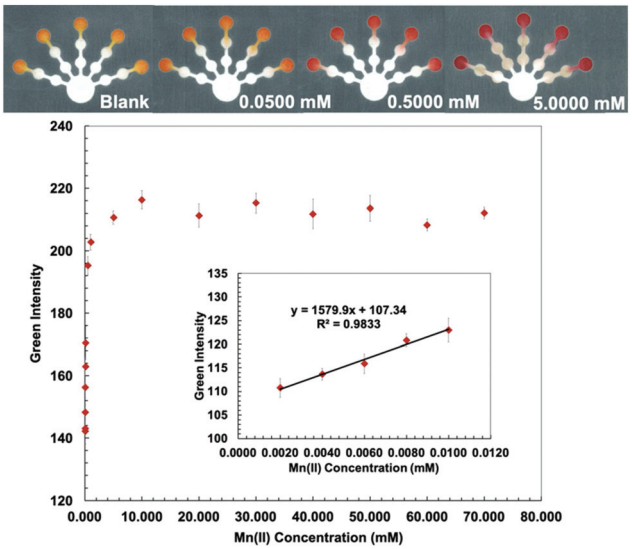

Fig. 5 Visual calibration curve was generated for semi-quantitative Mn (II) determination (top). Mn(II) calibration curve was produced in the range of 0.0020–0.0100 mM by analyzing the green intensity of the color change in the detection zone (bottom).

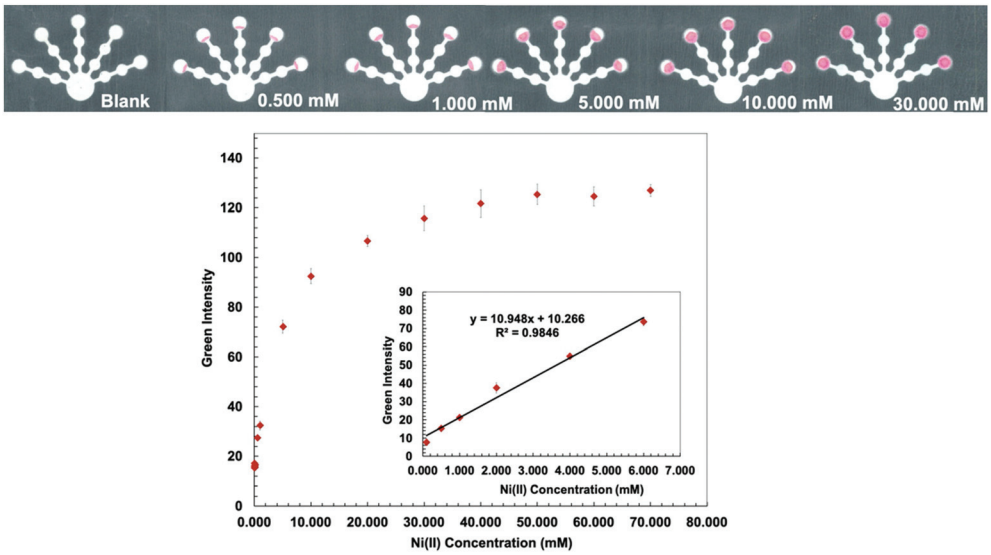

Fig. 6 Visual calibration curve was generated for semi-quantitative Ni(II) determination (top). Ni(II) calibration curve was produced in the range of 0.100–6.000 mM by analyzing the green intensity of the color change in the detection zone (bottom).

The proposed sensor performance was evaluated under the optimized conditions for each metal on a single device. The linear regression equation for each target metal ion reaction was determined by plotting the optimum color intensities and metal concentrations with $y = 28.317x + 8.2206$ ($R^2 = 0.9977$), $y = 256.73x + 118.5$ ($R^2 = 0.9887$), $y = 10.948x + 10.266$ ($R^2 = 0.9846$), $y = 850.11x + 82.884$ ($R^2 = 0.9831$), and $y = 1579.9x + 107.34$ ($R^2 = 0.9833$) for Cu(II), Co(II), Ni(II), Hg(II), and Mn(II) determination, respectively. The lowest detectable concentration, linear range, and saturated concentration for each metal ion are summarized in Table 1. The lowest detectable concentration of Cu(II) was lower than the regulation levels and that of Mn(II) was close to the regulation levels for heavy metal ions in drinking water.[4] The proposed sensor could be applied for simultaneous detection of the five metal ions in various water samples.

The device design was successfully applied for the quantification of Cu(II), Co(II), Ni(II), Hg(II), and Mn(II) using the reagent conditions for a single target metal on one device in which each detection zone serves as a replicate ($n = 5$). The design was also successfully applied for simultaneous screening of Cu(II), Co(II), Ni(II), Hg(II), and Mn(II) with the naked eye using the five optimized reagent conditions on a single device. After loading the pretreatment and detection zones with the appropriate reagents, a solution containing the five target metal ions (with varying metal ion concentrations) was added to the sample zone. The color change for each reaction on one device was recorded using a scanner after 120 min. The orange $Cu(Bc)_2$, pink $Ni(DMG)_2$, pink-red $Hg(DTZ)_2$, red $Co(PAR)_2$, and red $Mn(PAR)_2$ complexes are shown in Fig. 7. The proposed sensor showed high selectivity, efficiency, and portability for simultaneous screening of Cu(II), Co(II), Ni(II), Hg(II), and Mn(II) on one device with the naked eye.

The proposed sensor was successfully applied for simultaneous determination of Cu(II), Co(II), Ni(II), Hg(II), and Mn(II). The comparison of the performance between the proposed paper-based sensor and other paper-based sensors for heavy metal analysis by colorimetric methods is shown in Table 2. With the proposed sensor, more metals are detectable at once. In addition, the lowest detectable concentrations for Cu(II), Ni(II), and Hg(II) are lower than those reported in previous works. The linear range is wider for Cu(II) assay and Ni(II). The pro-

Table 1 Summary of the analytical performance of the proposed sensor for Cu(II), Co(II), Ni(II), Hg(II), and Mn(II) determination using the reagent conditions for a single target metal on one device ($n = 5$)

	Lowest detectable concentration (naked eye)		Color intensity					
			Lowest detectable concentration		Linear range		Saturated concentration	
Target metal ion	mM	mg L^{-1}	mM	mg L^{-1}	mM	mg L^{-1}	mM	mg L^{-1}
Cu(II)	0.050	3.18	0.005	0.32	0.005–1.000	0.32–63.55	40.0	2542
Co(II)	0.050	2.95	0.010	0.59	0.010–0.080	0.59–4.71	10.0	589
Ni(II)	0.500	29.35	0.100	5.87	0.100–6.000	5.87–352.16	40.0	2348
Hg(II)	0.050	10.03	0.001	0.20	0.001–0.060	0.20–12.04	1.0	201
Mn(II)	0.0500	2.75	0.0020	0.11	0.0020–0.0100	0.11–0.55	10	549

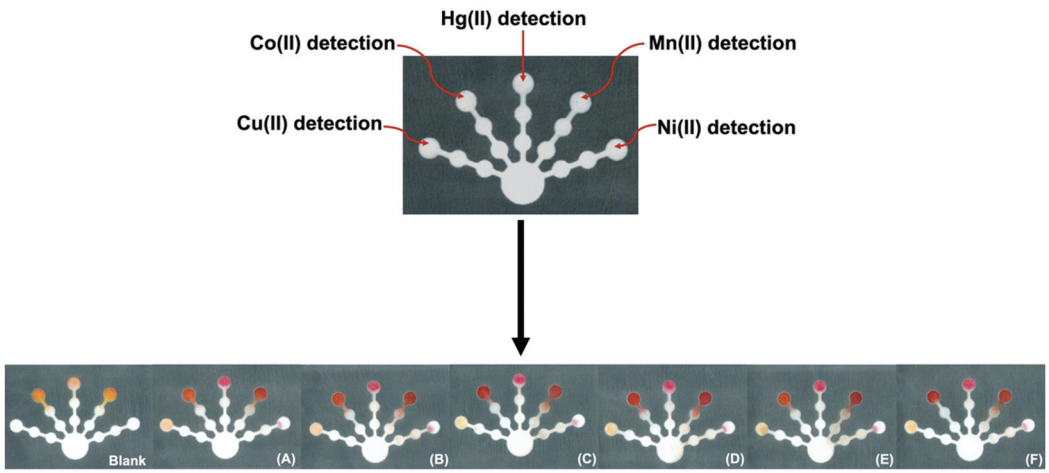

Fig. 7 The color change of the metal complexes for simultaneous detection of the five metal ions on one device of (A) 1 : 1 ratio for all five metal ions, (B) 1 : 2 for Cu(II) : other metal ions, (C) 1 : 2 for Co(II) : other metal ions, (D) 1 : 2 for Ni(II) : other metal ions, (E) 1 : 2 for Hg(II) : other metal ions, and (F) 1 : 2 for Mn(II) : other metal ions.

Table 2 Comparison of the performance between the proposed paper-based sensor and other paper-based sensors based on the wax printing fabrication method for heavy metal determination by colorimetric detection

Target metal ion	Lowest detectable concentration (mg L^{-1})	Complexing agent	Linear range (mg L^{-1})	Device design	Ref.
Cu(II)	0.32	Bathocuproine	0.32–63.55		This work
Co(II)	0.59	4-(2-Pyridylazo) resorcinol	0.59–4.71		
Ni(II)	5.87	Dimethylglyoxime	5.87–352.16		
Hg(II)	0.20	Dithizone	0.20–12.04		
Mn(II)	0.11	4-(2-Pyridylazo) resorcinol	0.11–0.55		
Cu(II)	15	Bathocuproine	60–300	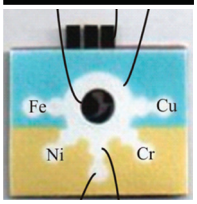	31
Ni(II)	15	Dimethylglyoxime	30–300		
Cr(VI)	2.4	1,5-Diphenylcarbazide	7.6–120		
Fe(III)	15	1,10-Phenanthroline	30–300		
Hg(II)	0.93	Dithizone	1–30	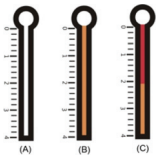	55
Fe(II)	20	4,7-Diphenyl-1-1,10-phenanthroline	100–1100	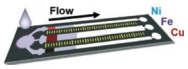	14
Ni(II)	100	Dimethylglyoxime	20–1300		
Cu(II)	100	Dithiooxamide	100–1300		
Cu(II)	1.60	Bathocuproine	5–80	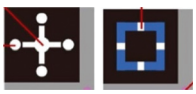	56
Ni(II)	4.80	Dimethylglyoxime	15–60		
Cr(VI)	0.18	1,5-Diphenylcarbazide	0.50–10		

posed device has a simple fabrication method, is easy to use and analyze, and can be applied for simultaneous screening and determination of the five metal ions in various environmental water samples.

Application of the proposed sensor for simultaneous determination of the five metal ions in real water samples

For Cu(II), Co(II), Ni(II), Hg(II), and Mn(II) determination in real water samples, the paper-based device was prepared under the

Table 3 Summary of the recovery test of the proposed sensor and the standard method (ICP-OES) for Cu(II), Co(II), Ni(II), Hg(II), and Mn(II) determination in drinking water

		Proposed sensor (n = 5)			ICP-OES (n = 3)		
Metal ion	Added (mM)	Found (mM)	%Recovery	%RSD	Found (mM)	%Recovery	%RSD
Cu(II)	—	N.D.			N.D.		
	0.080	0.086 ± 0.031	108	8.28	0.094 ± 0.001	118	0.35
	0.400	0.415 ± 0.034	104	4.82	0.434 ± 0.003	109	0.63
	0.800	0.834 ± 0.064	104	5.70	0.825 ± 0.008	103	0.99
Co(II)	—	N.D.			N.D.		
	0.020	0.020 ± 0.013	100	2.65	0.021 ± 0.001	105	1.36
	0.040	0.041 ± 0.016	103	3.19	0.042 ± 0.002	105	3.07
	0.060	0.063 ± 0.004	105	0.80	0.076 ± 0.001	127	1.81
Ni(II)	—	N.D.			N.D.		
	0.800	0.835 ± 0.077	104	4.34	0.786 ± 0.001	98	0.05
	2.000	2.145 ± 0.083	107	2.70	2.168 ± 0.003	108	0.14
	4.000	4.179 ± 0.186	104	3.63	4.092 ± 0.009	102	0.21
Hg(II)	—	N.D.			N.D.		
	0.008	0.008 ± 0.003	100	2.91	0.008 ± 0.001	100	1.57
	0.020	0.022 ± 0.003	110	2.49	0.020 ± 0.001	100	0.59
	0.040	0.044 ± 0.001	110	0.58	0.040 ± 0.001	100	0.19
Mn(II)	—	N.D.			N.D.		
	0.0040	0.0047 ± 0.0005	118	0.68	0.0049 ± 0.0003	123	2.90
	0.0060	0.0072 ± 0.0013	120	1.78	0.0071 ± 0.0001	118	2.29
	0.0080	0.0096 ± 0.0010	120	1.27	0.0087 ± 0.0001	109	0.69

N.D.: none detectable.

optimized reagent conditions for one metal at a time. The real water samples included drinking, tap, and pond water. Drinking water was obtained from a commercial product of Thailand. Tap and pond water were sampled from Chulalongkorn University. These samples were pretreated by filtration (0.45 μm) before use. Each target metal ion was spiked at three concentration levels in the three water samples. These samples were pH adjusted with pH 5 acetate buffer. For each concentration, each metal ion was spiked at the ratio of 1 : 1 for Cu(II), Co(II), Hg(II), and Mn(II) determination. Because Co(II) interferes with Ni(II), Ni(II) was spiked at three levels (0.800, 2.000, and 4.000 mM) while Cu(II), Hg(II), and Mn(II) were spiked at 0.910 mM and Co(II) was spiked at 0.455 mM. The recoveries and %RSD values were determined to be in the range of 91–109% and 1.98–8.28% (Cu(II)), 100–120% and 0.80–3.48% (Co(II)), 101–107% and 2.58–5.49% (Ni(II)),

Table 4 Summary of the recovery test of the proposed sensor and the standard method (ICP-OES) for Cu(II), Co(II), Ni(II), Hg(II), and Mn(II) determination in tap water

		Proposed sensor (n = 5)			ICP-OES (n = 3)		
Metal ion	Added (mM)	Found (mM)	%Recovery	%RSD	Found (mM)	%Recovery	%RSD
Cu(II)	—	N.D.			N.D.		
	0.080	0.073 ± 0.021	91	5.69	0.093 ± 0.002	116	0.83
	0.400	0.410 ± 0.037	103	5.24	0.427 ± 0.002	107	1.45
	0.800	0.756 ± 0.021	95	1.98	0.805 ± 0.009	101	0.60
Co(II)	—	N.D.			N.D.		
	0.020	0.024 ± 0.004	120	0.83	0.021 ± 0.001	105	4.16
	0.040	0.047 ± 0.011	118	2.25	0.040 ± 0.001	100	5.61
	0.060	0.067 ± 0.018	112	3.48	0.058 ± 0.001	97	2.82
Ni(II)	—	N.D.			N.D.		
	0.800	0.856 ± 0.057	107	3.19	0.778 ± 0.002	97	0.10
	2.000	2.135 ± 0.082	107	2.68	2.145 ± 0.006	107	0.29
	4.000	4.056 ± 0.129	101	2.58	4.033 ± 0.016	101	0.29
Hg(II)	—	N.D.			N.D.		
	0.008	0.009 ± 0.001	113	1.86	0.008 ± 0.001	100	0.08
	0.020	0.022 ± 0.003	110	1.19	0.019 ± 0.001	95	0.30
	0.040	0.044 ± 0.003	110	2.25	0.040 ± 0.002	100	0.22
Mn(II)	—	0.0047 ± 0.0026			0.0014 ± 0.0002		
	0.0040	0.0092 ± 0.0012	113	1.61	0.0061 ± 0.0001	117	1.13
	0.0060	0.0114 ± 0.0023	112	2.92	0.0078 ± 0.0001	107	1.30
	0.0080	0.0139 ± 0.0013	115	1.55	0.0098 ± 0.0002	105	1.04

N.D.: none detectable.

Table 5 Summary of the recovery test of the proposed sensor and the standard method (ICP-OES) for Cu(II), Co(II), Ni(II), Hg(II), and Mn(II) determination in pond water

		Proposed sensor (n = 5)			ICP-OES (n = 3)		
Metal ion	Added (mM)	Found (mM)	%Recovery	%RSD	Found (mM)	%Recovery	%RSD
Cu(II)	—	N.D.			N.D.		
	0.080	0.081 ± 0.023	101	6.30	0.090 ± 0.001	113	0.46
	0.400	0.434 ± 0.035	109	4.87	0.417 ± 0.004	104	0.87
	0.800	0.748 ± 0.024	94	2.36	0.792 ± 0.006	99	0.81
Co(II)	—	N.D.			N.D.		
	0.020	0.022 ± 0.015	110	3.03	0.022 ± 0.001	110	4.16
	0.040	0.044 ± 0.012	110	2.31	0.039 ± 0.001	98	5.61
	0.060	0.066 ± 0.013	110	2.46	0.058 ± 0.001	97	2.82
Ni(II)	—	N.D.			N.D.		
	0.800	0.839 ± 0.098	105	5.49	0.786 ± 0.001	98	0.01
	2.000	2.128 ± 0.121	106	3.94	2.154 ± 0.004	108	0.27
	4.000	4.218 ± 0.157	105	3.05	4.087 ± 0.018	102	0.50
Hg(II)	—	N.D.			N.D.		
	0.008	0.008 ± 0.005	100	3.45	0.008 ± 0.001	100	1.68
	0.020	0.022 ± 0.006	110	4.46	0.022 ± 0.001	110	1.79
	0.040	0.044 ± 0.003	110	4.63	0.043 ± 0.001	108	0.91
Mn(II)	—	N.D.			N.D.		
	0.0040	0.0050 ± 0.0007	125	1.02	0.0045 ± 0.0001	113	2.15
	0.0060	0.0074 ± 0.0022	123	2.89	0.0067 ± 0.0003	112	2.80
	0.0080	0.0099 ± 0.0017	124	2.22	0.0084 ± 0.0004	105	3.13

N.D.: none detectable.

100–113% and 0.58–4.63% (Hg(II)), and 112–125% and 0.68–2.92% (Mn(II)) for drinking, tap, and pond waters (Tables 3–5). The accuracy of the proposed sensor was validated by the standard ICP-OES method with no significant difference (paired *t*-test, 95% confidence interval).[57] The precision of the proposed method was evaluated using a single set of reagent conditions on a paper device and by measuring the color intensity of each target metal ion (0.455 mM) on three devices on the same day (n = 15). The relative standard deviations (RSDs) were in the range of 3.98–5.77% (Cu(II)), 1.69–3.21% (Co(II)), 1.46–4.79% (Ni(II)), 2.08–4.66% (Hg(II)), and 1.39–2.29% (Mn(II)). The proposed method showed acceptable accuracy and precision in accordance with The Association of Official Analytical Chemists (AOAC).[58]

Conclusion

A paper-based sensor was designed for simultaneous quantification of Cu(II), Co(II), Ni(II), Co(II), and Mn(II) using a set of five optimized reagent conditions on one device. The metals were detected by a colorimetric reaction between the metal ions and complexing agents in each detection zone. In addition, the device design consisted of two pretreatment zones with masking agents to increase the specificity for the metals by removing the interfering ions. The orange $Cu(Bc)_2$, pink $Ni(DMG)_2$, pink-red $Hg(DTZ)_2$, red $Co(PAR)_2$, and red Mn $(PAR)_2$ complexes demonstrated high selectivity for simultaneous analysis of Cu(II), Co(II), Ni(II), Hg(II), and Mn(II). The optimal conditions were determined to achieve the lowest detectable concentrations of 0.005 mM (0.32 mg L^{-1}), 0.010 mM (0.59 mg L^{-1}), 0.100 mM (5.87 mg L^{-1}), 0.001 mM (0.20 mg L^{-1}), and 0.0020 mM (0.11 mg L^{-1}) for Cu(II), Co(II), Ni(II), Hg(II), and Mn(II) determination, respectively. The lowest detectable concentration of Cu(II) was lower than the regulation levels and that of Mn(II) was close to the regulation levels for heavy metal ions in drinking water.[4] The analytical performance was evaluated in three types of water samples. The results obtained from the proposed paper-based sensor were compared to the results obtained by the standard ICP-OES method with good accuracy and precision. This proposed paper-based sensor demonstrated its utility for highly selective, sensitive, low cost, and simultaneous detection of Cu (II), Co(II), Ni(II), Hg(II), and Mn(II) in real water samples with the naked eye.

Author contributions

Pornphimon Kamnoet: conceptualization, methodology, investigation, data analysis, formal analysis, writing-original draft. Wanlapa Aeungmaitrepirom: supervision, conceptualization, writing-review & editing. Ruth F. Menger: conceptualization, reviewing and editing. Charles S. Henry: supervision, conceptualization, writing-review & editing.

Conflicts of interest

There is no conflict to declare.

Acknowledgements

This research was financially supported by the Development and Promotion of Science and Technology Talents Project (Royal Government of Thailand scholarship) under Henry Group (Colorado State University, United States) and Environmental Analysis Research Unit (Chulalongkorn University, Thailand). The device was partially fabricated by Electrochemistry and Optical Spectroscopy Research Unit (EOSRU), Department of Chemistry, Faculty of Science, Chulalongkorn University, Patumwan, Bangkok 10330, Thailand. CSH and RFM acknowledge the support from the National Institutes of Health through R43 ES031906-01.

References

1 X. Qu, W. Xu, J. Ren, X. Zhao, Y. Li and X. Gu, *J. Hazard. Mater.*, 2020, **400**, 123135.
2 H. G. Hoang, C. Lin, H. T. Tran, C. F. Chiang, X. T. Bui, N. K. Cheruiyot, C. C. Shern and C. W. Lee, *Environ. Technol. Innovation*, 2020, **20**, 101043.
3 M. Jaishankar, T. Tseten, N. Anbalagan, B. B. Mathew and K. N. Beeregowda, *Interdiscip. Toxicol.*, 2014, **7**, 60–72.
4 Pollution Control Department, MNRE Thailand, *MNRE Decree on Industrial Effluent Standard B.E. 2016, Thailand*, 2016.
5 Y. Liu, D. Xue, W. Li, C. Li and B. Wan, *Microchem. J.*, 2020, **158**, 105221.
6 L. C. Almeida, J. B. da Silva Junior, I. F. Dos Santos, V. S. de Carvalho, A. de Santana Santos, G. M. Hadlich and S. L. C. Ferreira, *Mar. Pollut. Bull.*, 2020, **158**, 111423.
7 L. Nyaba and P. N. Nomngongo, *Food Chem.*, 2020, **322**, 126749.
8 S. Hamida, L. Ouabdesslam, A. F. Ladjel, M. Escudero and J. Anzano, *Anal. Lett.*, 2018, **51**, 2501–2508.
9 S. R. N. Endah and S. I. Surantaatmadja, *J. Phys.: Conf. Ser.*, 2019, **1179**, 12178.
10 M. Lo, A. K. D. Diaw, D. Gningue-Sall, M. A. Oturan, M. M. Chehimi and J. J. Aaron, *Luminescence*, 2019, **34**, 489–499.
11 W. Huang, Y. Zhang, Y. Li, T. Zeng, Q. Wan and N. Yang, *Anal. Chim. Acta*, 2020, **1126**, 63–71.
12 X. Xin, N. Hu, Y. Ma, Y. Wang, L. Hou, H. Zhang and Z. Han, *Dalton Trans.*, 2020, **49**, 4570–4577.
13 A. Faridan, M. Bahmae and A. M. Sharif, *Anal. Bioanal. Electrochem.*, 2020, **12**, 810–827.
14 D. M. Cate, S. D. Noblitt, J. Volckens and C. S. Henry, *Lab Chip*, 2015, **15**, 2808–2818.
15 J. C. Jokerst, J. M. Emory and C. S. Henry, *Analyst*, 2012, **137**, 24–34.

16 S. Chaiyo, W. Siangphroh, A. Apilux and O. Chailapakul, *Anal. Chim. Acta*, 2015, **866**, 75–83.
17 P. Rattanarat, W. Dungchai, D. M. Cate, W. Siangproh, J. Volckens, O. Chailapakul and C. S. Henry, *Anal. Chim. Acta*, 2013, **800**, 50–55.
18 Y. Lu, W. Shi, L. Jiang, J. Qin and B. Lin, *Electrophoresis*, 2009, **30**, 1497–1500.
19 P. J. Bracher, M. Gupta, E. T. Mack and G. M. Whitesides, *ACS Appl. Mater. Interfaces*, 2009, **1**, 1807–1812.
20 A. W. Martinez, S. T. Phillips, B. J. Wiley, M. Gupta and G. M. Whitesides, *Lab Chip*, 2008, **8**, 2146–2150.
21 A. W. Martinez, *Bioanalysis*, 2011, **3**, 2589–2592.
22 W. Dungchai, O. Chailapakul and C. S. Henry, *Analyst*, 2011, **136**, 77–82.
23 S. Chaiyo, A. Apiluk, W. Siangproh and O. Chailapakul, *Sens. Actuators, B*, 2016, **233**, 540–549.
24 K. R. Chabaud, J. L. Thomas, M. N. Torres, S. Oliveira and B. R. McCord, *Forensic Chem.*, 2018, **9**, 35–41.
25 P. Teengam, W. Siangproh, A. Tuantranont, T. Vilaivan, O. Chailapakul and C. S. Henry, *Anal. Chem.*, 2017, **89**, 5428–5435.
26 E. Carrilho, W. A. Martinez and M. G. Whitesides, *Anal. Chem.*, 2009, **81**, 7091–7095.
27 M. L. Firdaus, A. Aprian, N. Meileza, M. Hitsmi, R. Elvia, L. Rahmidar and R. Khaydarov, *Chemosensors*, 2019, **7**, 35–41.
28 H. Sharifi, J. Tashkhourian and B. Hemmateenejad, *Anal. Chim. Acta*, 2020, **1126**, 114–123.
29 S. Muhammad-Aree and S. Teepoo, *Anal. Bioanal. Chem.*, 2020, **412**, 1395–1405.
30 R.-E. Dong, P. Kang, X.-L. Xu, L.-X. Cai and Z. Guo, *Sens. Actuators, B*, 2020, **312**, 128013.
31 P. Rattanarat, W. Dungchai, D. Cate, J. Volckens, O. Chailapakul and C. S. Henry, *Anal. Chem.*, 2014, **86**, 3555–3562.
32 H. Wang, L. Yang, S. Chu, B. Liu, Q. Zhang, L. Zou, S. Yu and C. Jiang, *Anal. Chem.*, 2019, **91**, 9292–9299.
33 H. Iwai, *Anal. Sci.*, 2017, **33**, 1231–1236.
34 S. A. R. Soares, S. S. L. Costa, R. G. O. Araujo, L. S. G. Teixeira and A. F. Dantas, *J. AOAC Int.*, 2018, **101**, 876–882.
35 J. Palmer, *Plymouth Stud. Sci.*, 2014, **7**, 151–184.
36 M. M. Mentele, J. Cunningham, K. Koehler, J. Volckens and C. S. Henry, *Anal. Chem.*, 2012, **84**, 4474–4480.
37 G. Britain, *Talanta*, 1973, **20**, 228–232.
38 A. Shahat, E. A. Ali and M. F. El Shahat, *Sens. Actuators, B*, 2015, **221**, 1027–1034.
39 R. P. Paradkar and R. R. Williams, *Anal. Chem.*, 1994, **66**, 2752–2756.
40 N. A. Azmi, S. H. Ahmad and S. C. Low, *RSC Adv.*, 2018, **8**, 251–261.
41 D. Wilkins and F. Smith, *Anal. Chim. Acta*, 1953, **9**, 338–348.
42 Y. Zhang, J. Jiang, M. Li, P. Gao, L. Shi, G. Zhang, C. Dong and S. Shuang, *Sens. Actuators, B*, 2017, **238**, 683–692.
43 *Electrolytes, EFM, and Chemical equilibrium*, https://drjvazque.files.wordpress.com/2012/2001/tablas-de-formacion-de-complejos.
44 J. Zhai and E. Bakker, *Analyst*, 2016, **141**, 4252–4261.
45 G. Chakrapani, D. S. R. Murty, B. K. Balaji and R. Rangawamy, *Talanta*, 1993, **40**, 541–544.
46 R. Pribil and V. Vesely, *Talanta*, 1961, **8**, 270–275.
47 C. M. Doyle, D. Naser, H. A. Bauman, J. A. O. Rumfeldt and E. M. Meiering, *Anal. Biochem.*, 2019, **579**, 44–56.
48 X. Zhou, J. Nie and B. Du, *ACS Appl. Mater. Interfaces*, 2015, **7**, 21966–21974.
49 N. A. Meredith, J. Volckens and C. S. Henry, *Anal. Methods*, 2017, **9**, 534–540.
50 N. Raoot and S. Raoot, *Talanta*, 1981, **28**, 327–328.
51 L. E. Godycki and R. E. Rundle, *Acta Crystallogr.*, 1953, **6**, 487.
52 B. Ebrahimi, S. Bahar and S. E. Moedi, *J. Braz. Chem. Soc.*, 2013, **24**, 1832–1839.
53 A. Izquierdo, *Polyhedron*, 1986, **5**, 1007–1011.
54 D. B. Gazda, J. S. Fritz and M. D. Porter, *Anal. Chem.*, 2004, **76**, 4881–4887.
55 X. Li, D. R. Ballerini and W. Shen, *Biomicrofluidics*, 2012, **6**, 85214.
56 X. Sun, B. Li, A. Qi, C. Tian, J. Han, Y. Shi, B. Lin and L. Chen, *Talanta*, 2018, **178**, 426–431.
57 M. Senila, A. Drolc, A. Pintar, L. Senila and E. Levei, *Anal. Sci. Technol.*, 2014, **5**, 37.
58 AOAC International, *Appendix K: Guidelines for Dietary Supplements and Botanicals, Part I*, 2013.